*Pure Appl. Chem.*, Vol. 83, No. 10, pp. 1819–1830, 2011.
doi:10.1351/PAC-REP-11-01-10


# Morphology development of polytetrafluoroethylene in a polypropylene melt (IUPAC Technical Report)*

Mohd Amran Bin Md Ali, Shogo Nobukawa, and Masayuki Yamaguchi‡

*School of Materials Science, Japan Advanced Institute of Science and Technology, 1-1 Asahidai, Nomi, Ishikawa 923-1292 Japan*

*Abstract*: Morphology development of polytetrafluoroethylene (PTFE) caused by applied flow history in molten isotactic polypropylene (PP) is investigated, employing a cone-and-plate rheometer and a capillary rheometer as mixing devices. Since the flow history is applied at 190 °C, PTFE is in the solid state whereas PP is in the molten state. It is found that primary PTFE particles tend to be agglomerated together by mechanical interlocking. Then they are fragmented into fibers by hydrodynamic force with reorganization process of crystalline phase. The diameter of the fragmented fibers is the same as that of the original ellipsoidal particles. Further, fine fibers whose diameter is in the range from 50 to 100 nm are also generated by yielding behavior of the particles. The prolonged shearing leads to a large number of fibers, although the diameter and length are hardly affected by the exposure time of shearing and shear stress. Moreover, the flow type (i.e., drag or pressure flow) does not affect the morphology to a great extent, although the drag flow is not efficient to reduce large agglomerated particles. The fibers form an interdigitated network structure, which is responsible for the marked melt elasticity.

*Keywords*: IUPAC Polymer Division; morphology; nanofibers; polymer blends; polytetrafluoroethylene; rheology.

## INTRODUCTION

Polytetrafluoroethylene (PTFE) shows a lot of interesting properties such as high melting point, marked resistance to solvent, low yield stress, and low surface tension [1]. It has been known that PTFE has two transition temperatures in the solid state at approximately 19 and 30 °C [2–6]. Below 19 °C, shearing will make PTFE particles slide past each other, retaining their identity. Around 19 °C, PTFE exhibits a first-order transition from triclinic to hexagonal crystalline form. The cohesive force between neighbor chains in the hexagonal crystalline lattice is not strong [7–11]. Consequently, the packed PTFE molecules in the crystalline form are unwound by a low level of shear force, leading to fibrils. In particular, fibrillation occurs easily beyond 30 °C even in the solid state [12,13]. Furthermore, Ariawan et al. investigated the morphology development of PTFE during paste flow in an extrusion die and found that PTFE particles are interconnected together and turned into a fibrous shape [14]. Meanwhile, recent

*Sponsoring body: IUPAC Polymer Division: see more details on page 1829.

‡Corresponding author: Tel.: +81-761-51-1621; Fax +81-761-51-1625; E-mail: m_yama@jaist.ac.jp

studies proved that PTFE can be used as a processing modifier for isotactic polypropylene (PP), because it improves the melt elasticity [15–18], one of the most serious problems for conventional PP [19–26]. According to our previous paper [15], blending a small amount of PTFE enhances the storage modulus in the low-frequency region and normal stress difference. Moreover, drawdown force, defined as a force needed for extension of a molten strand, is improved to a great extent, which is required at various processing operations. It should be noted that the rheological modification is attained by existence of "solid" PTFE, because the rheological measurements were performed at lower temperature than the melting point of PTFE. Furthermore, morphology observation by a scanning electron microscope (SEM) revealed that PTFE exists as fine fibers whose diameter is smaller than 500 nm in a molten PP. Therefore, it can be concluded that flexible fine fibers, which will form an interdigitated network structure, are responsible for the marked melt elasticity. These experimental results have been supported also by another research group [16–18]. Further, they demonstrated that the blend of PP with PTFE shows marked strain-hardening behavior in uniaxial elongational viscosity, one of the most important elastic properties for polymer processing operations such as foaming, thermoforming, and blow-molding. Since the interdigitated structure of PTFE fibers in a molten PP will be responsible for the attractive rheological properties, it must be significantly important to control the size and shape of the fibers. To the best of our knowledge, however, morphology development of PTFE in a molten polymer has not been examined yet in spite of the great performance as a processing modifier. Moreover, this new type of a polymer composite/blend containing polymeric nanofibers with high melting point can widen the application of polymeric materials because of the improved processability. Considering that extensive study has been carried out to prepare various nanofibers recently, polymer composites with nanofibers will be available without any difficulty as already demonstrated by several researchers [27–32]. The rheological properties must be significantly different from those of conventional polymer composites containing large fibers such as kenaf, coir-coconut, jute, bamboo, hemp, and wood fibers [33–38].

Finally, it was found that the rheological properties and processability of the polymer composite containing PTFE fibers are dependent on the processing history to a great extent [15], which is similar to shear modification behavior of long-chain branched polymers [39–42]. The change of shape and dispersion state of PTFE fibers during processing would affect the rheological properties. Therefore, the morphology development of PTFE in a molten PP has to be understood in detail to control the processability.

In this study, the morphology development of solid PTFE particles in a molten PP is investigated. For the purpose, drag shear flow by a cone-and-plate rheometer and pressure-driven shear flow by a capillary rheometer are applied to PP containing PTFE particles in the temperature range between the melting points of the polymers.

## EXPERIMENTAL

### Materials

The polymers used in this study were PTFE and isotactic PP. PP is a commercially available propylene homopolymer (Japan Polypropylene, Novatec-PP FY4), and PTFE powder was kindly supplied by Mitsubishi Rayon. The melt flow index of PP is 5 [g/10 min] at 230 °C, and the melting point is 165 °C. The characteristics of PTFE are described in detail later. Prior to mixing, PP was ground into powder form by a mill machine (Osaka Chemical Co. Ltd., PLC-2M) at room temperature.

### Sample preparation

PP powder was mixed with PTFE powder by manual operation at room temperature. The blend ratio was PP/PTFE (95/5) in weight fraction. The mixed powders were compressed into a flat sheet by a compression-molding machine at 220 °C under 10 MPa for 3 min and then subsequently cooled down at

30 °C. The thickness of the sheets was 1 mm. The compressed sheets were used to examine the effect of drag flow in a cone-and-plate rheometer on the morphology development of PTFE. The mixed powders were also employed to investigate the morphology development under pressure flow employing a capillary rheometer.

### Measurements

The morphology development under drag shear flow was studied employing a cone-and-plate rheometer (UBM, MR-500) as a function of exposure time of shearing at a constant shear rate, 5 $s^{-1}$. Further, the morphology development at various shear rates with a constant residence time, 5 min, was also studied. The diameter of the cone was 40 mm, and the cone angle was 5º. The experiments were performed at 190 °C under a nitrogen atmosphere to avoid thermal-oxidative degradation.

The effect of pressure-driven shear flow on the morphology development was studied at various shear rates using a capillary rheometer (Yasuda Seiki Seisakusyo, 140 SAS-2002). The temperature was controlled at 190 °C. The dimensions of the circular capillary dies employed were as follows; the length was 10 or 40 mm, the diameter was 1 mm, and the entrance angle was 180º.

The morphology of PTFE was examined by an SEM (Hitachi, S400) after surface-coating by Pt-Pd. In the case of the observation of PTFE fraction in the blends, the blend samples were put in a metal-mesh bag and dissolved in hot xylene for 3 h at 140 °C. Then the undissolved part in the metal-mesh bag was collected. The pore size of the metal mesh was 25 μm. The dissolution process was carried out twice to remove the PP fraction perfectly. Prior to the surface-coating, the undissolved part (i.e., PTFE) was dried in a vacuum oven.

Thermal analysis was conducted by a differential scanning calorimeter (DSC) (Mettler, DSC820) under a nitrogen atmosphere. The amount of the sample in an aluminum pan was approximately 10 mg in weight. The samples were heated in a nitrogen atmosphere from 25 to 350 °C at a heating rate of 10 °C/min as a first run. Then the sample was kept at 350 °C for 3 min to eliminate the thermal history. The sample was cooled down to 25 °C at a rate of 3 °C/min. After holding 3 min at 25 °C, the sample was heated again at the same heating rate, 10 °C/min, as a second run.

## RESULTS AND DISCUSSION

### Characteristics of PTFE

Prior to the evaluation of the blend samples, the thermal properties and morphology of the original PTFE powder are investigated. Figure 1 shows the DSC heating curves of the original PTFE powder at a heating rate of 10 °C/min. The melting point of the PTFE powder at the first scan is detected at 346 °C with a shoulder around 340 °C. At the second scan after the cooling process, the PTFE powder shows a sharp melting curve with a melting point at 327 °C. The results suggest that PTFE particles after polymerization have thick crystalline lamellae with a high melting point. Further, the cooling rate at the experiment (i.e., 3 °C/min) is too fast to grow thick lamellae for PTFE. A similar result was reported by Gangal [43]. According to him, the degree of crystallization of PTFE is sensitive to cooling condition and always decreases with increasing the cooling rate.

Figure 2a shows the SEM picture of the original PTFE powder. It was found that the primary particles of PTFE, which are in ellipsoidal shape, were agglomerated together. The average size of the primary particles is approximately 200 nm in diameter and 400 nm in length.

 

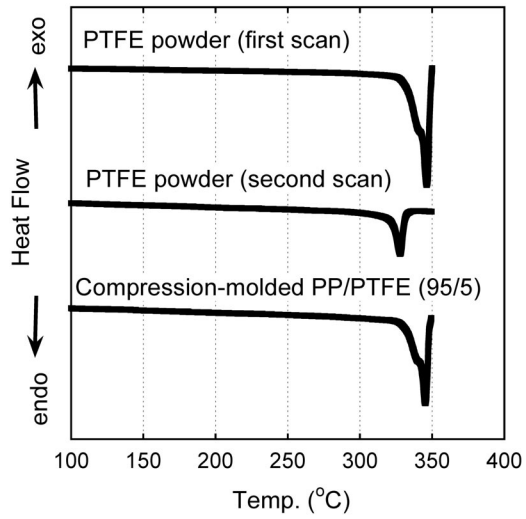


**Fig. 1** DSC heating curves for the original PTFE powder (first and second scans) and PTFE in the compression-molded sample of PP/PTFE (95/5). The heating rate is 10 °C/min.

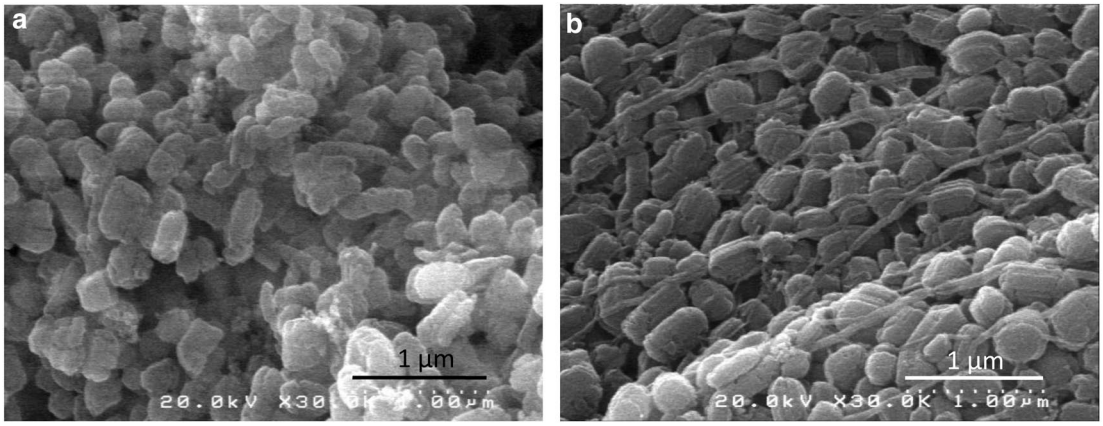


**Fig. 2** SEM pictures for (a) the original PTFE powder and (b) the undissolved part in the compression-molded sheet of PP/PTFE (95/5).

## Effect of compression-molding on the morphology of PTFE in a molten PP

The DSC heating curve of the residue in a metal-mesh bag after dissolution in hot xylene employing a compression-molded sample containing 5 wt % of PTFE is also shown in Fig. 1. As seen in the figure, the curve is almost identical to the first scan of the original PTFE powder, indicating that the compression-molding at the present condition has no/little effect on the crystalline state of PTFE. Further, a melting peak of PP was not detected, suggesting that PP fraction was dissolved in hot xylene and escaped from the metal-mesh bag perfectly.

Figure 2b shows the SEM picture of the undissolved part of the compression-molded sheet. Similar to Fig. 2a, a lot of the primary particles are detected even after the dissolution process by hot xylene. Considering that the PTFE fraction remains in the metal-mesh bag without passing through the pores of the metal-mesh, the primary particles must be connected together. The immiscible nature between PP and PTFE is responsible for the segregation of PTFE from a PP melt and thus the agglom-

eration. Further, the particles will be connected together during the storage of the powders after polymerization. Moreover, it should be noted that some PTFE particles are deformed into a fibrous shape owing to the applied squeeze flow as well as the localized shear deformation. The diameter of the fibers is smaller than 100 nm, and the length is longer than 2 μm. Therefore, the aspect ratio is larger than 20.

## Morphology development under drag flow

The effect of the applied drag flow on the morphology development of PTFE was studied employing the compression-molded films. Figure 3 shows DSC heating curves of PTFE fraction in the blends having various residence times in the cone-and-plate rheometer at a constant shear rate of 5 $s^{-1}$. In the figure, the heating curve of the sample obtained by the compression-molding without shearing is denoted as "0 min". Therefore, the curve is identical to that in Fig. 1 (i.e., the compression-molded sample). It is found from the curves that the melting point and its heat of fusion depend on the shear history, although the experiments are performed at 190 °C (i.e., lower than the melting point of PTFE).

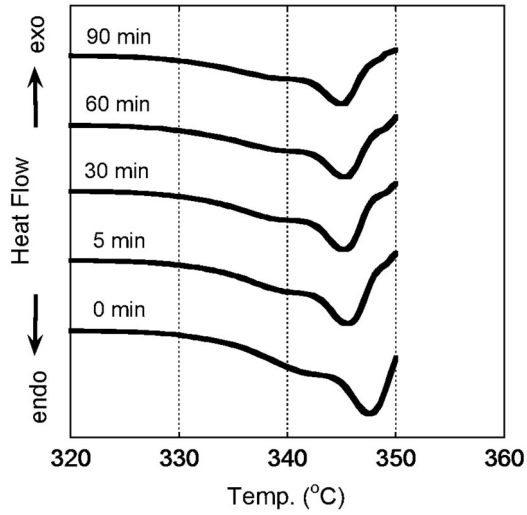


**Fig. 3** DSC heating curves of PTFE in PP/PTFE (95/5) blend having shear history at 5 $s^{-1}$ for various times. The heating rate is 10 °C/min.

As seen in Fig. 4, the heat of fusion $\Delta H$ of PTFE decreases with increasing the exposure time of shearing. Furthermore, the melting point also decreases with the prolonged shear history. The heat of fusion for the compressed film (i.e., 0 min) is about 68 J/g and that for the sample sheared for 90 min is about 58 J/g. Assuming that the heat of fusion of perfect crystals is 82 J/g [44], the degree of crystallinity is calculated to be 83 % for "0 min" and 72 % for "90 min". The mechanical energy applied by shearing destroys and/or melts the crystallites of PTFE to some degree, which is attributed to the low level of cohesive force in PTFE crystals.

 

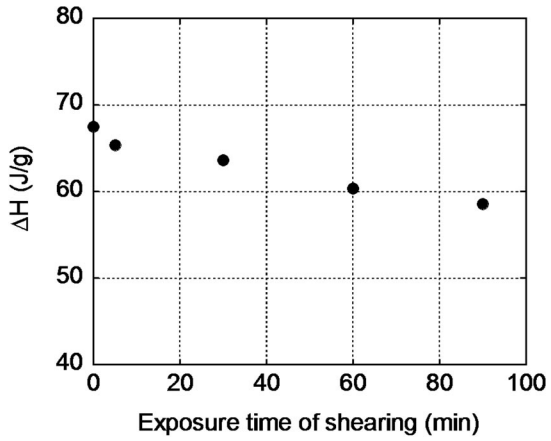


**Fig. 4** Heat of fusion of PTFE in Fig. 3 as a function of exposure time of shearing.

Figure 5 shows the growth curves of shear stress for a compressed sheet of PP/PTFE (95/5) at various shear rates. As seen in the figure, the shear stress of the sample is almost a constant at any shear rate in the experimental range. Therefore, it can be regarded as a steady-state shear stress from the viewpoints of mechanical response, although it should be noted that the morphology is developing in the cone-and-plate rheometer as shown later. The steady-state shear stress is plotted in Fig. 6 as a function of the shear rate. The solid line in the figure represents the shear stress for pure PP, which is almost similar to those for PP/PTFE (95/5). The result indicates that a small amount of PTFE does not affect the shear stress.

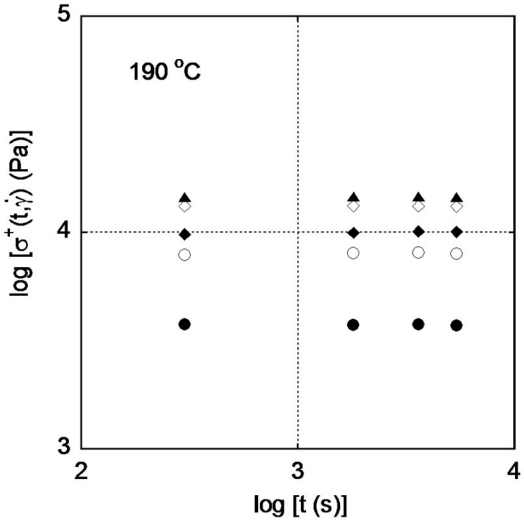


**Fig. 5** Growth curves of shear stress $\sigma^{+}(t)$ at various shear rates as a function of exposure time of shearing at 190 °C for PP/PTFE (95/5) blend. The shear rates $\dot{\gamma}$ were (closed circles) 1 $s^{-1}$, (open circles) 3 $s^{-1}$, (closed diamonds) 5 $s^{-1}$, (open diamonds) 10 $s^{-1}$, and (closed triangles) 20 $s^{-1}$.

 

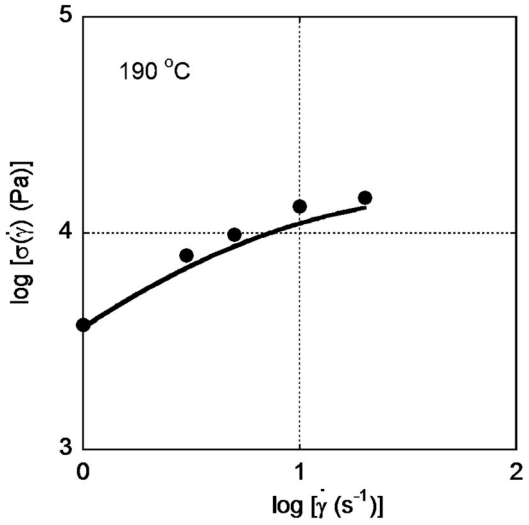


**Fig. 6** Shear stress $\sigma$ plotted against the shear rate $\dot{\gamma}$ at 190 °C for (closed symbols) PP/PTFE (95/5) blend and (solid line) pure PP.

Figure 7 shows the SEM pictures of PTFE in the blend samples having shear histories at 5 $s^{-1}$. When the shear flow is applied for 5 min, as shown in Fig. 7a, agglomerated primary particles with some fibers are detected as a sheet in the residue. On the contrary, after long residence time (e.g., 60 min), most of the residues are in fibrous shape as shown in Fig. 7b.

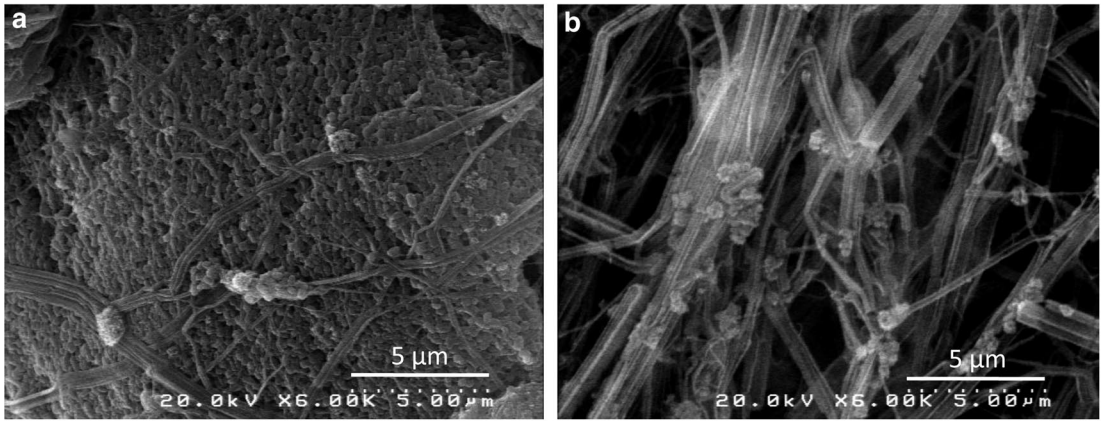


**Fig. 7** SEM pictures of PTFE in PP/PTFE (95/5) blend after applied shear history by the cone-and-plate rheometer at 5 $s^{-1}$ for (a) 5 min and (b) 60 min.

Figure 7 also demonstrates that the diameter of most PTFE fibers, which is independent of the exposure time of shearing, is approximately 200 nm. This is the same size as the diameter of the primary particles, although some fine fibers are also detected. Furthermore, the mechanical interlocked structure can be observed in the sheared sample as exemplified in Fig. 8. The arrows in the figure will be the boundary between primary particles. Considering that a large sheet composed of agglomerated particles is detected in the compression-molded sample, the fibers are generated by the fragmentation

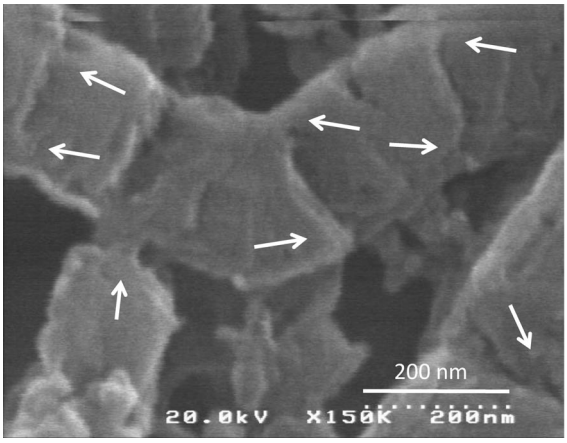


**Fig. 8** Magnified SEM picture of PTFE in PP/PTFE (95/5) blend after applied shear history by the cone-and-plate rheometer at 5 $s^{-1}$ for 60 min.

of the sheet by applied shear stress in the rheometer. During the fragmentation process, the degree of crystallization in the surface of primary particles decreases to some degree as shown in Fig. 4.

These results indicate that there are two types of fibers; one is obtained by large plastic deformation of a primary particle, leading to fine fibers with small diameter. The other is generated by the fragmentation of agglomerated particles connected by mechanical interlocking. The diameter of the fibers obtained by the latter mechanism is almost the same as that of the primary particles.

The number of fibers per unit area is calculated from SEM pictures. It is found to be 1.4 [fibers/$\mu m^2$] for the sample having shear flow at 5 $s^{-1}$ for 60 min and 1.0 [fibers/$\mu m^2$] for the compression-molded one. This result suggests that almost all of the fine fibers are generated at the initial compression-molding process. Intensive squeeze force at compression-molding would be responsible for the yielding and then deformation of primary particles.

Figure 9 shows the undissolved part of the blend at different shear rates for 5 min. It is found from the figure that large chunks of agglomerated particles are detected at a low shear rate (i.e., low shear stress). On the contrary, more fibers are detected at a high shear rate, although the diameter of individ-

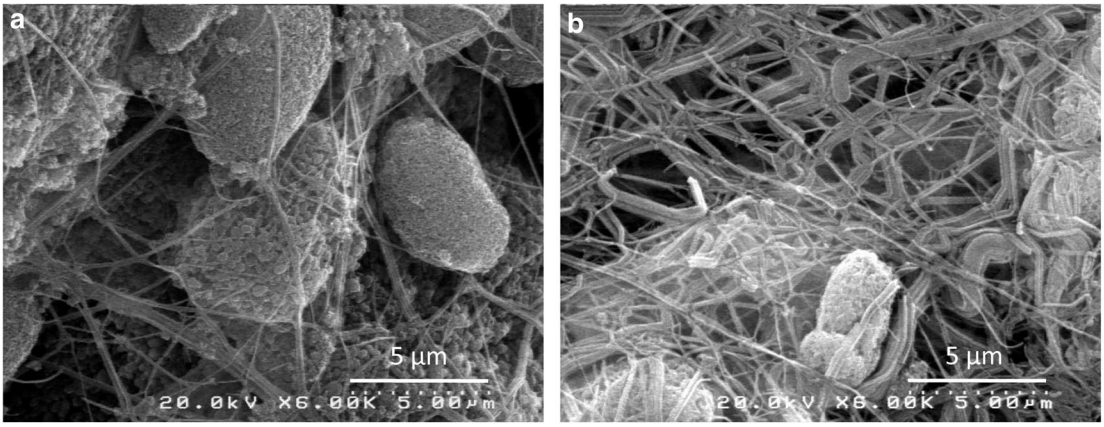


**Fig. 9** SEM pictures of PTFE in PP/PTFE (95/5) blend after applied shear history by the cone-and-plate rheometer for 5 min at (a) 1 $s^{-1}$ and (b) 10 $s^{-1}$.

ual fibers is not affected by the shear rate. It suggests that a high level of shear stress is preferred to reduce the large agglomeration of PTFE particles in the blend.

### Morphology development under pressure flow

In order to clarify the morphology development of PTFE under a pressure flow, the capillary extrusion of powder blends composed of PP and PTFE is performed, employing a capillary rheometer at various shear rates at 190 °C. Figure 10 shows the shear stress plotted against the shear rate as compared with the data of pure PP without Bagley and Rabinowitch corrections. The difference in the values between Figs. 10 and 6 would be owing to the end-pressure drop. As seen in the figure, the apparent wall shear stress of the blends is almost identical to that of pure PP in the experimental shear rate region, as similar to that in the low shear rate region shown in Fig. 6.

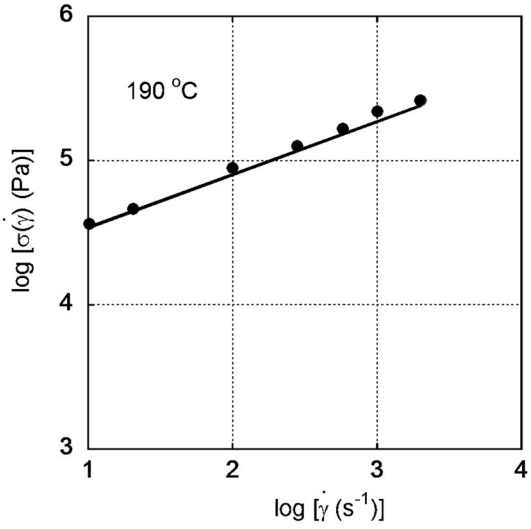


**Fig. 10** Shear rate $\dot{\gamma}$ dependence of shear stress $\sigma$ measured by the capillary rheometer with a circular die having L/D = 10/1 (mm) at 190 °C for (closed symbols) PP/PTFE (95/5) blend and (solid line) pure PP.

Figure 11 shows the undissolved part of the strand extruded by a capillary rheometer at a shear rate of 10 $s^{-1}$, employing two circular dies with different length. Since both dies have the same diameter, the average residence time in the longer die (44 s) is four times as long as that in the shorter die (11 s). As seen in Fig. 11a, the PTFE particles are agglomerated together with few fibers. On the contrary, it is found that a lot of particles are deformed into nanofibers in the sample extruded by the longer die. The results demonstrate that the formation of fibers increases with increasing the residence time under shear.

 

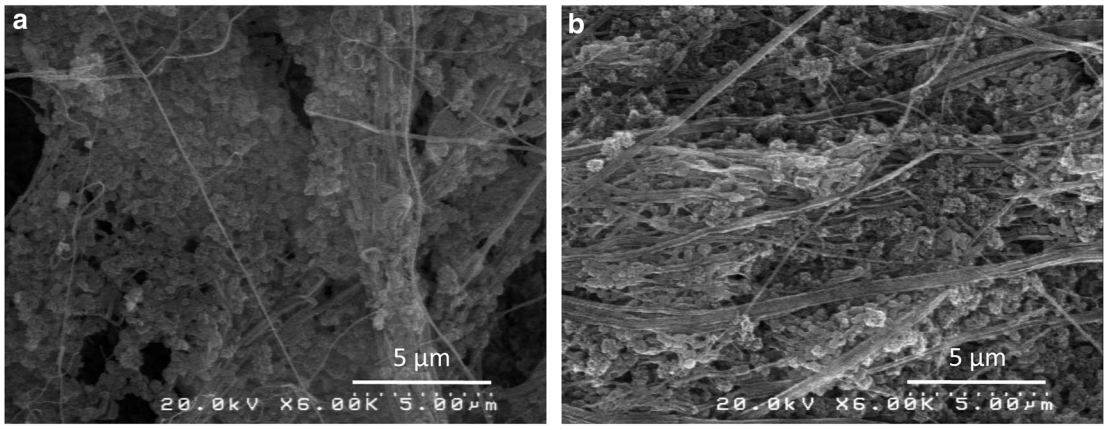


**Fig. 11** SEM pictures of PTFE in PP/PTFE (95/5) blend extruded by the capillary rheometer at 190 °C at 10 $s^{-1}$. The dimensions of the dies are (a) L/D = 10/1 (mm) and (b) L/D = 40/1 (mm).

Further, as compared with Fig. 9b, the effect of flow type (i.e., drag or pressure flow) on the morphology development can be discussed. It is found that the diameter of fibers in the blend obtained under the pressure flow is about 200 nm, similar to that of fibers obtained under the drag flow. Moreover, large agglomerated particles are detected in the samples obtained by the drag flow. Considering that the residence time in the capillary die is much shorter than that in the cone-and-plate rheometer, the pressure flow seems to be effective to destroy the agglomeration. Finally, it is found that large chunks of agglomerated particles almost disappear at a shear rate of 2000 $s^{-1}$. However, as seen in Fig. 12b, primary particles are still detected between fibers, suggesting that longer residence time and/or higher shear stress are required to obtain the ideal morphology (i.e., no primary particle).

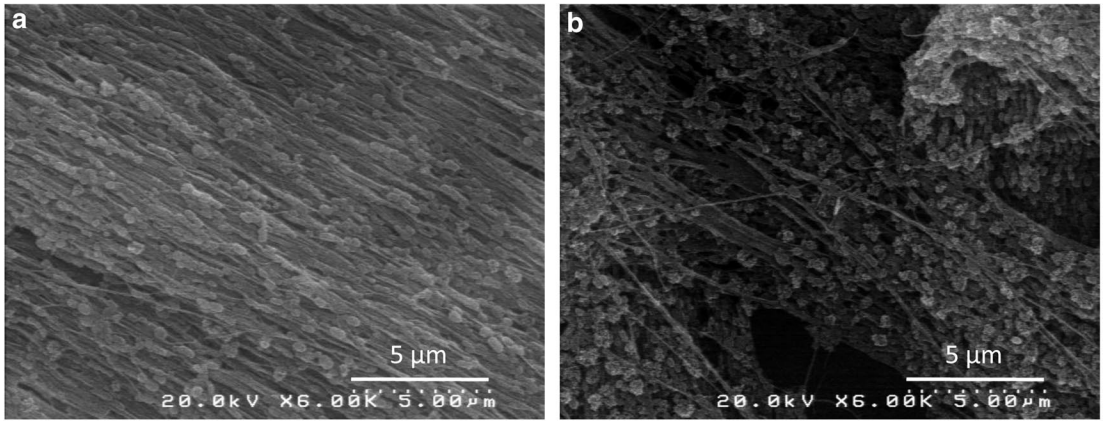


**Fig. 12** SEM pictures of PTFE in PP/PTFE (95/5) blend at a shear rate of 2000 $s^{-1}$. The lengths of dies are for (a) 40 mm and (b) 10 mm.

## CONCLUSION

Morphology development of solid PTFE particles in a molten PP is studied, employing a cone-and-plate rheometer and a capillary rheometer as mixing devices. The shear flow is applied at 190 °C (i.e., lower than the melting point of PTFE). It is found that almost all of the PTFE particles, which are in ellip-

soidal shape after polymerization, are deformed into fibrous shape by applied shear history. Because of the incompatibility with PP, PTFE particles are excluded from a molten PP and agglomerated each other. The connected particles are then fragmentated into fibers by the applied shear stress with fusion of PTFE crystals to some degree. Since the diameter of the fibers is the same as that of the initial particles, the fibers are considered to be composed of one-dimensional connection of the primary particles. The loose packing of crystalline chains of PTFE is responsible for the unique morphology development in a molten PP. Further, it is also found that the diameter of some fibers is in the range between 50 and 100 nm. The fine fibers are mainly generated by compression-molding. Because of the intensive squeeze force, primary particles show plastic deformation, leading to fine fibers. In our experimental results, however, the number of fine fibers is independent of the shear stress, the exposure time of shearing, and the type of shear flow (i.e., drag or pressure flow). Considering that the interdigitated network composed of the flexible nanofibers in a molten PP is responsible for a high level of melt elasticity such as Barus effect, normal stress difference, and strain-hardening in elongational viscosity, the experimental results obtained in this study will be important information to control the rheological properties as well as the processability.

## MEMBERSHIP OF SPONSORING BODIES

Membership of the IUPAC Polymer Division Committee for the period 2010–2011 was as follows:

***President*:** C. K. Ober (USA); ***Vice President*:** M. Buback (Germany); ***Secretary*:** M. Hess (Germany); ***Titular Members*:** D. J. Dijkstra (Germany); R. G. Jones (UK); P. Kubisa (Poland); G. T. Russell (Germany); M. Sawamoto (Japan); R. F. T. Stepto (UK); J.-P. Vairon (France); ***Associate Members*:** D. Berek (Slovakia); J. He (China); R. C. Hiorns (France); W. Mormann (Germany); D. W. Smith (USA); J. Stejskal (Czech Republic); ***National Representatives*:** K.-N. Chen (Taiwan); J.-S. Kim (Korea); G. Moad (Australia); M. Raza Shah (Pakistan); J. V. Seppälä (Finland); R. P. Singh (India); W. M. Z. B. Wan Yunus (Malaysia); Y. Yagci (Turkey); M. Zigon (Slovenia).

## ACKNOWLEDGMENTS

The authors acknowledge the IUPAC project (No. 2010-029-3-400) for the collection of samples. The authors are also grateful to Mitsubishi Rayon Co. Ltd. for their kind advice.

## REFERENCES

1. D. L. Kerbow. In *Polymer Data Handbook*, J. E. Mark (Ed.), pp. 842–847, Oxford University Press, Oxford (1999).
2. C. W. Burn, E. R. Howells. *Nature* **174**, 569 (1954).
3. C. A. Sperati, H. W. Starkweather. *Adv. Polym. Sci.* **2**, 465 (1961).
4. S. Mazur. In *Polymer Powder Technology*, M. Narkis (Ed.), pp. 441–481, John Wiley, New York (1995).
5. D. L. Kerbow, C. A. Sperati. In *Polymer Handbook*, J. Bandrup, E. H. Immergut (Eds.), pp. V/31–V58, John Wiley, New York (1989).
6. P. Rachele. *J. Fluorine Chem.* **125**, 293 (2004).
7. E. S. Clark, L. T. Muus. *Krist.* **117**, 119 (1962).
8. C. M. Sharts. *J. Chem. Educ.* **45**, 185 (1968).
9. T. A. Blanchet. In *Handbook of Thermoplastics*, O. Olabisi (Ed.), pp. 981–1000, Marcel Dekker, New York (1997).
10. E. N. Brown, D. N. Dattelbaum. *Polymer* **46**, 3056 (2005).
11. L. S. Schandler, L. C. Brinson, W. G. Sawyer. *Nanocompos. Mater. JOM* 50 (2007).
12. J. G. Drobny. *Technology of Flouropolymers*, CRC Press, Boca Raton (2008).

 

13. S. Ebnesajjad. *Fluoroplastics, Vol. 1: Non-Melt Processible Fluoroplastics*, Plastics Design Library, New York (2000).
14. A. B. Ariawan, S. Ebnesajjad, S. G. Hatzikiriakos. *Can. J. Chem. Eng.* **80**, 1153 (2002).
15. M. A. B. M. Ali, K. Okamoto, M. Yamaguchi, T. Kasai, A. Koshirai. *J. Polym. Sci., Polym. Phys.* **47**, 2008 (2009).
16. T. Murata, J. Takimoto, K. Koyama. *Polym. J.* **45**, 1300 (1996).
17. T. Kurose, T. Takahashi, K. Koyama. *Polym. J.* **31**, 195 (2003).
18. T. Kurose, T. Takahashi, M. Sugimoto, T. Taniguchi, K. Koyama. *Polym. J.* **33**, 178 (2005).
19. R. Hingmann, B. L. Marczinke. *J. Rheol.* **38**, 573 (1994).
20. C. B. Park, L. K. Cheung. *Polym. Eng. Sci.* **37**, 1 (1997).
21. H. C. Lau, S. N. Bhattacharya, G. Field. *Polym. Eng. Sci.* **38**, 1915 (1998).
22. M. Yamaguchi, M. H. Wagner. *Polymer* **47**, 3629 (2006).
23. M. Yamaguchi, H. Miyata. *Polym. J.* **32**, 164 (2000).
24. M. Yamaguchi. *J. Polym. Sci., Polym. Phys.* **39**, 228 (2001).
25. M. Yamaguchi. *ANTEC* 1149 (2001).
26. M. Yamaguchi. In *Polymeric Foams: Mechanisms and Materials*, S. T. Lee, N. S. Ramesh (Eds.), Chap. 2, CRC Press, Boca Raton (2004).
27. G. I. Taylor. *Proc. R. Soc. London A* **138**, 41 (1932).
28. N. Tokita, I. Pliskin. *Rub. Chem. Technol.* **46**, 1166 (1973).
29. H. P. Grace. *Chem. Eng. Commun.* **14**, 225 (1982).
30. S. Wu. *Polym. Eng. Sci.* **27**, 335 (1987).
31. H. E. H. Meijer, J. M. H. Janssen, P. D. Anderson. In *Mixing and Compounding of Polymers*, Z. I. Manas-Zloczower, A. Tadmor (Eds.), pp. 41–177, Hanser, Munich (1994).
32. T. Yokohara, M. Yamaguchi. *Eur. Polym. J.* **44**, 677 (2008).
33. H. Gao, Y. M. Song, Q. W. Wang, Z. Han, M. I. Zhang. *J. For. Res.* **19**, 315 (2008).
34. S. Mohanty, S. K. Verma, S. K. Nayak. *J. Appl. Polym. Sci.* **99**, 1476 (2006).
35. M. J. A. van den Oever, M. H. B. Snijder. *J. Appl. Polym. Sci.* **110**, 1009 (2008).
36. I. Ghasemi, H. Azizi, N. Naeimian. *Iran. Polym. J.* **17**, 191 (2008).
37. E. T. Twite-Kabamba, A. Mechraoui, D. Rodrique. *Polym. Compos.* **30**, 1401 (2009).
38. Z. Y. Chen, W. H. Yan, Q. Y. Ping. *Bioresour. Technol.* **101**, 7944 (2010).
39. H. Münstedt, H. M. Laun. *Rheol. Acta* **20**, 211 (1981).
40. M. Yamaguchi, C. G. Gogos. *Adv. Polym. Technol.* **20**, 261 (2001).
41. M. Yamaguchi, D. B. Todd, C. G. Gogos. *Adv. Polym. Technol.* **22**, 179 (2003).
42. K. Ono, M. Yamaguchi. *J. Appl. Polym. Sci.* **113**, 1462 (2009).
43. S. V. Gangal. In *Encyclopedia of Chemical Technology*, pp. 621–644, John Wiley, New York (1994).
44. S. F. Lau, H. Suzuki, B. Wunderlich. *J. Polym. Sci., Polym. Phys.* **22**, 379 (1984).